NASA MEMO 10-22-58L

NASA

MEMORANDUM

LOW-SPEED STATIC STABILITY CHARACTERISTICS OF TWO CONFIGURATIONS SUITABLE FOR LIFTING REENTRY FROM SATELLITE ORBIT

By John W. Paulson

Langley Research Center
Langley Field, Va.

NATIONAL AERONAUTICS AND SPACE ADMINISTRATION
WASHINGTON
November 1958
Declassified April 12, 1961

1Z

NATIONAL AERONAUTICS AND SPACE ADMINISTRATION

NASA MEMO 10-22-58L

LOW-SPEED STATIC STABILITY CHARACTERISTICS OF TWO CONFIGURATIONS SUITABLE FOR LIFTING REENTRY FROM SATELLITE ORBIT*

By John W. Paulson

SUMMARY

An investigation of the low-speed static stability and control characteristics of 1/4-scale models of two configurations suitable for lifting reentry from satellite orbit has been made in the Langley free-flight tunnel. One of the models was a thick, all-wing configuration having a delta plan form and the other was a flat delta wing with a half-cone fuselage.

The investigation showed that, in general, the all-wing configuration had better longitudinal and lateral stability characteristics than the flat delta configuration.

INTRODUCTION

An investigation is being conducted by the National Aeronautics and Space Administration to provide information on the stability and control characteristics of some configurations suitable for lifting reentry from satellite orbit over the range from low-subsonic to hypersonic speeds. The present investigation was made to provide some information at low-subsonic speeds on the longitudinal and lateral stability characteristics of 1/4-scale models of a thick, all-wing configuration having a delta plan form (model 1) and a configuration having a flat delta wing with a half-cone fuselage (model 2).

This study included static force tests at angles of attack from 0° to 90° to determine the longitudinal characteristics and tests at constant angle of attack over a sideslip range of $\pm 20^{\circ}$ to determine the lateral characteristics. The flat-delta-wing configuration was tested in both the erect and inverted positions to determine whether having the fuselage on the top or bottom of the wing had any effect on the

*Title, Unclassified.

longitudinal characteristics. The effect on the longitudinal characteristics of deflecting the forward portion of the models up 20° was also determined. All tests were made with the controls at 0° deflection.

SYMBOLS

The longitudinal data are referred to the stability system of axes and the lateral data are referred to the body system of axes. (See fig. 1.) The origin of the axes was located to correspond to a longitudinal center-of-gravity position at 39 percent of the mean aerodynamic chord for both models. This center-of-gravity position gave about neutral longitudinal stability in the low angle-of-attack range for both models.

S	wing area, sq ft
$\bar{c}$	wing mean aerodynamic chord, ft
V	airspeed, ft/sec
b	wing span, ft
q	dynamic pressure, $\frac{\rho V^2}{2}$, lb/sq ft
ρ	air density, slugs/cu ft
β	angle of sideslip, deg
α	angle of attack, deg
R	radius of curvature
F_L	lift force, lb
F_D	drag force, lb
F_Y	side force, lb
M_Y	pitching moment, ft-lb
M_X	rolling moment, ft-lb
M_Z	yawing moment, ft-lb

C_L lift coefficient, F_L/qS

C_D drag coefficient, F_D/qS

C_m pitching-moment coefficient, $M_Y/qS\bar{c}$

C_n yawing-moment coefficient, M_Z/qSb

C_l rolling-moment coefficient, M_X/qSb

C_Y lateral-force coefficient, F_Y/qS

$C_{n_\beta} = \frac{\partial C_n}{\partial \beta}$ per degree

$C_{l_\beta} = \frac{\partial C_l}{\partial \beta}$ per degree

$C_{Y_\beta} = \frac{\partial C_Y}{\partial \beta}$ per degree

δ_N deflection of forward portion of model, positive when nose is up, deg

APPARATUS AND MODELS

The models were tested in the Langley free-flight tunnel, which is a low-speed tunnel with a 12-foot octagonal test section. A sting-type support system and an internally mounted three-component strain-gage balance were used.

The investigation was made with 1/4-scale models. Three-view drawings of the models used in the investigation are presented in figure 2, and the dimensions are given in table I. The all-wing model was modified for some tests by the addition of a transition strip. The strips investigated included a 0.125-inch zig-zag rod and a 0.5-inch-wide roughness strip having particles with a maximum diameter of 0.06 inch. The models were also modified so that the forward portion could be deflected up 20°. This deflected portion amounted to 30 and 20 percent of the root chord for models 1 and 2, respectively.

TESTS

Force tests were made to determine the static longitudinal and lateral stability characteristics of the models over an angle-of-attack range from 0° to 90° with 0° control deflection. Model 2 was tested in both the erect and inverted positions to determine whether the longitudinal characteristics were affected by having the fuselage on the top or the bottom. Tests were also made to determine the effect on the longitudinal characteristics of deflecting the forward portion of the models up 20° (see fig. 2) to improve the trim characteristics. The lateral characteristics were determined from runs made at various angles of attack over a sideslip range of ±20°.

Model 1 was also tested with the transition fixed in order to duplicate more closely the full-scale characteristics. The proper location of the transition strips was determined by the fluorescent-oil-film technique developed at the Langley Laboratory. Force tests were made to determine the longitudinal characteristics of the model with two of the transition strips that evolved during the oil-film studies.

The lateral and longitudinal tests were run at dynamic pressures of 2.4 and 4.3 pounds per square foot, respectively. These dynamic pressures correspond to airspeeds of 45 and 60 feet per second. These velocities gave test Reynolds numbers of 1,037,000 and 1,380,000 based on the mean aerodynamic chord of 3.61 feet for model 1 and 1,135,000 and 1,510,000 based on the mean aerodynamic chord of 3.95 feet for model 2.

RESULTS AND DISCUSSION

Longitudinal Characteristics

The longitudinal characteristics of model 1 are presented in figure 3. From these data it may be seen that the maximum lift coefficient occurred at an angle of attack of 40° and the model had about neutral longitudinal stability up to this angle. The data of figure 3 also show that the maximum lift coefficient was increased by the 0.06-inch roughness transition strip and was decreased by the 0.125-inch zig-zag transition rod. The results obtained with the zig-zag rod are believed to be most representative of higher-scale data. The data show that the transition strips had fairly large effects on the drag and pitching-moment characteristics at some angles of attack. The data of figure 4 show that deflecting the forward portion of model 1 up 20° produced a positive pitching moment up to an angle of attack of 45° and increased the lift and drag but did not greatly affect the longitudinal stability.

The aerodynamic characteristics of model 2 in both the erect and inverted positions are presented in figure 5. The data show that the inverted configuration had a slightly higher lift-curve slope and higher maximum lift and also had better longitudinal stability and trim characteristics up to an angle of attack of 30°.

The data of figure 6 show that deflecting the forward portion of model 2 up 20° produced a positive pitching moment up to an angle of attack of about 50° and decreased the lift, increased the drag, and reduced the longitudinal stability. A comparison of the data in figure 6 with those in figure 4 shows that model 1 had generally better longitudinal characteristics than model 2.

Lateral Characteristics

The variation of the coefficients C_Y, C_n, and C_l with angle of sideslip for various angles of attack is shown in figure 7 for model 1 and in figure 8 for model 2. These data are summarized in figure 9 in the form of the stability derivatives C_{Y_β}, C_{n_β}, and C_{l_β} plotted against angle of attack. The values of the derivatives were obtained by measuring the slope between sideslip angles of 5° and -5°. The data of figure 9 show that both models were generally directionally stable over the unstalled part of the angle-of-attack range except at angles of attack from about 20° to 30°, where model 2 was unstable. Both models had positive effective dihedral over the entire angle-of-attack range tested. The values of these derivatives, particularly C_{n_β}, are not considered to give a very reliable indication of the stability over certain portions of the angle-of-attack range for the two models because of nonlinearities in the data of figures 7 and 8.

Langley Research Center,
National Aeronautics and Space Administration,
Langley Field, Va., July 7, 1958.

TABLE I

DIMENSIONAL CHARACTERISTICS OF THE MODELS

	Model 1	Model 2
Airfoil section	Wedge	Flat plate
Area (includes cutouts), sq ft	9.73	9.80
Span, ft	3.21	2.75
Aspect ratio	1.06	0.77
Root chord, ft	5.18	5.78
Tip chord, ft	0	0.95
Mean aerodynamic chord, ft	3.61	3.95
Sweepback of leading edge, deg	70	75
Dihedral	0	0

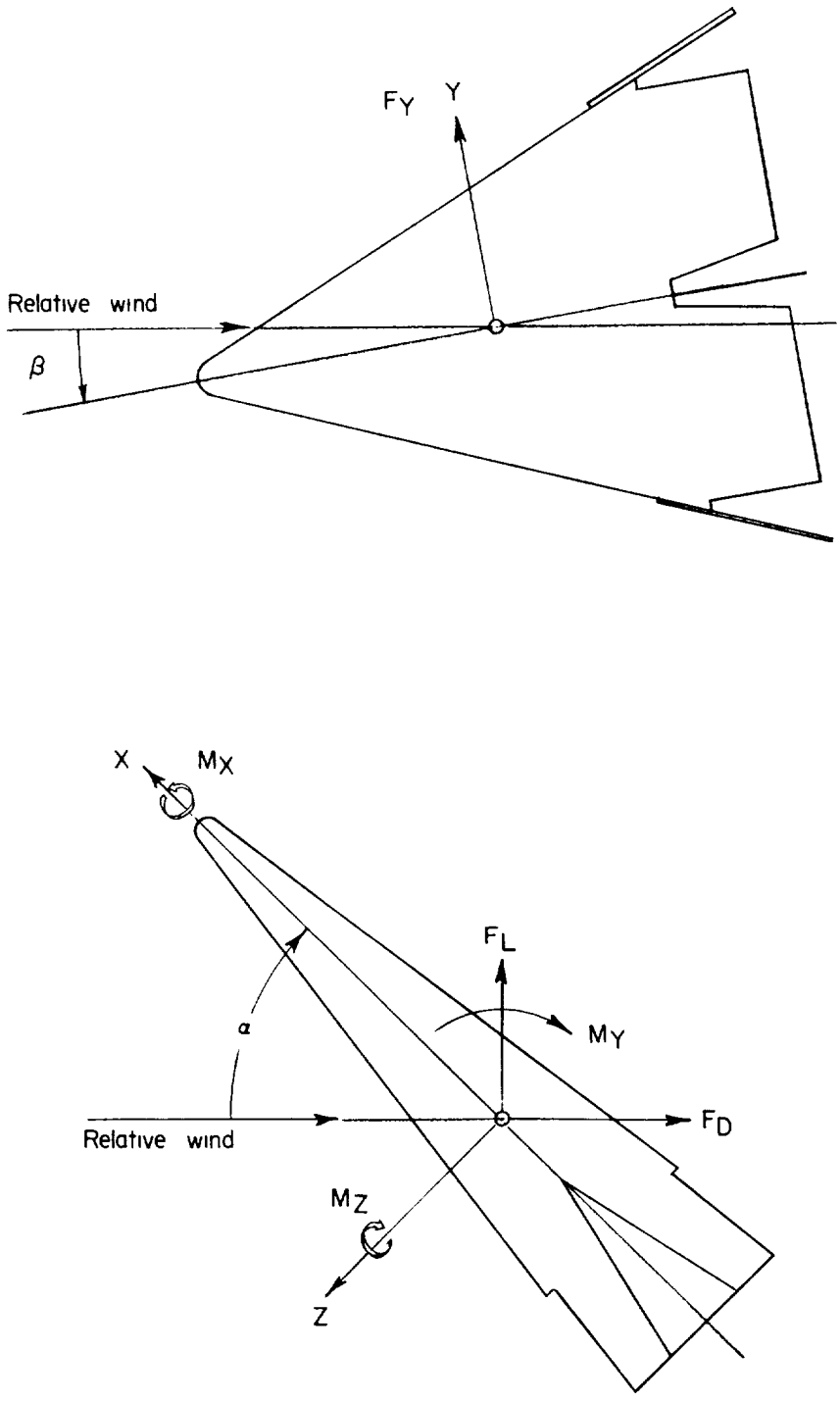

Figure 1.- Sketch of axis system showing positive direction of forces, moments, and angles.

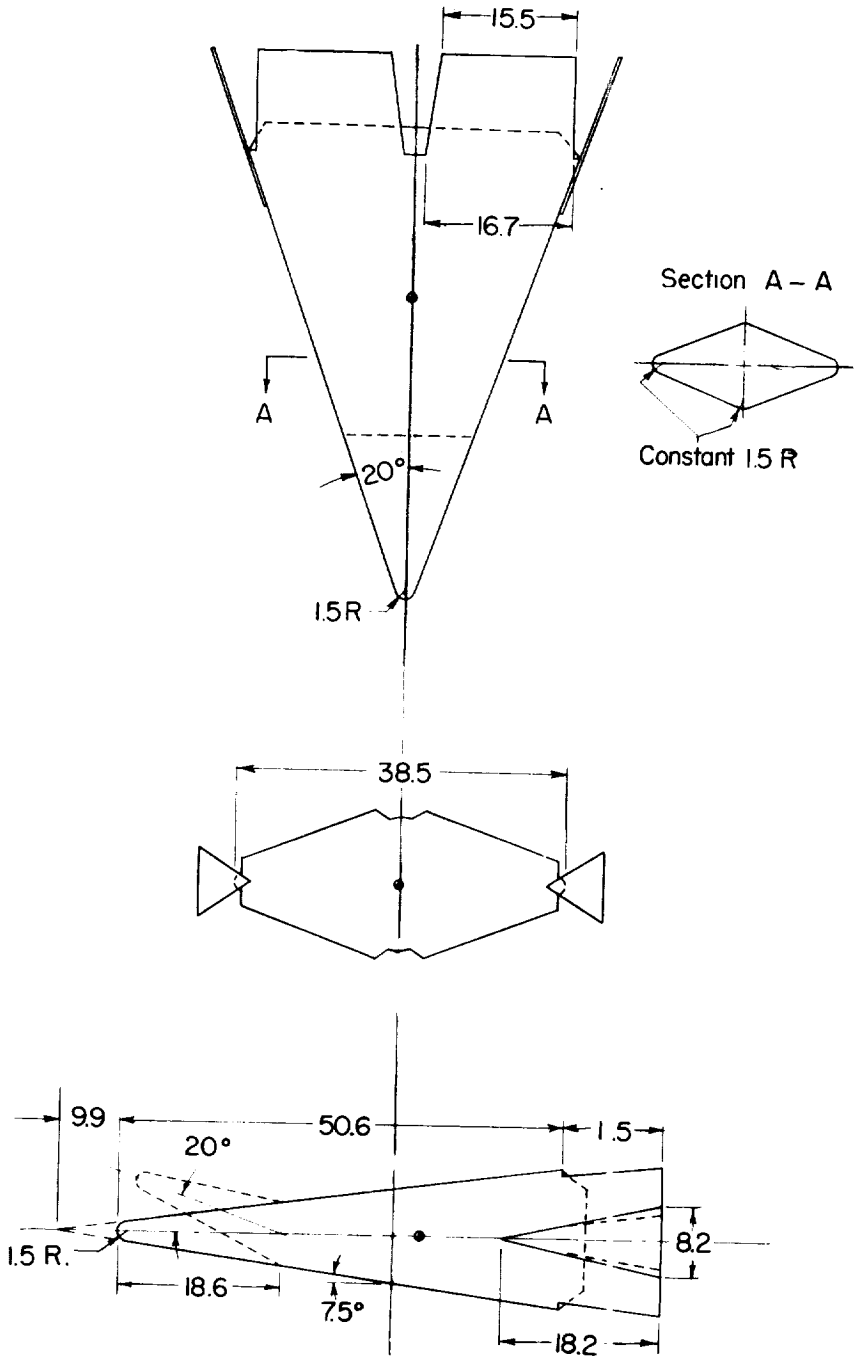

(a) Model 1.

Figure 2.- Three-view drawing of models used in investigation. All dimensions are in inches.

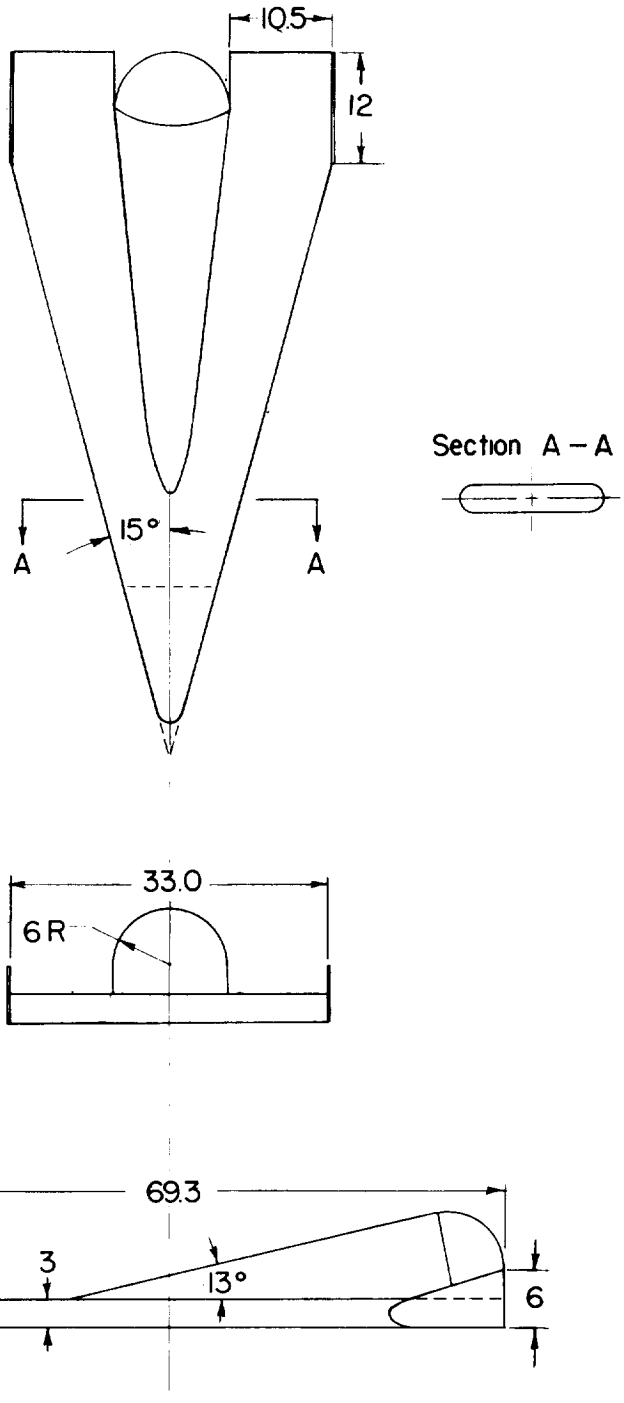

(b) Model 2.

Figure 2.- Continued.

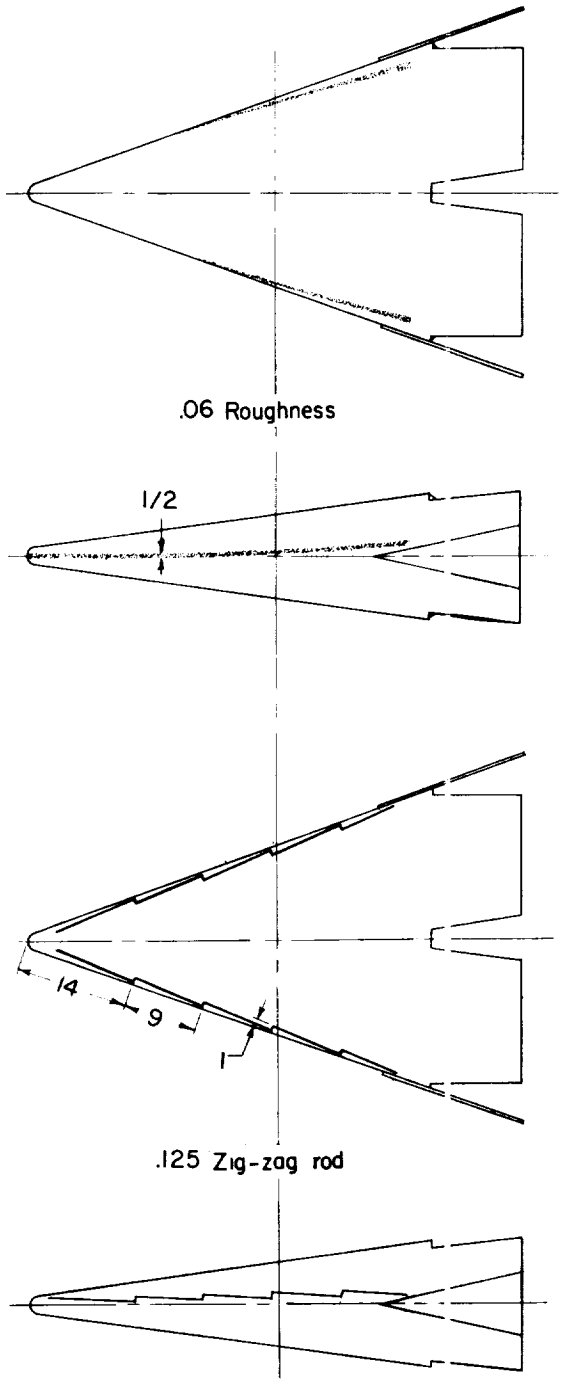

(c) Transition-strip location.

Figure 2.- Concluded.

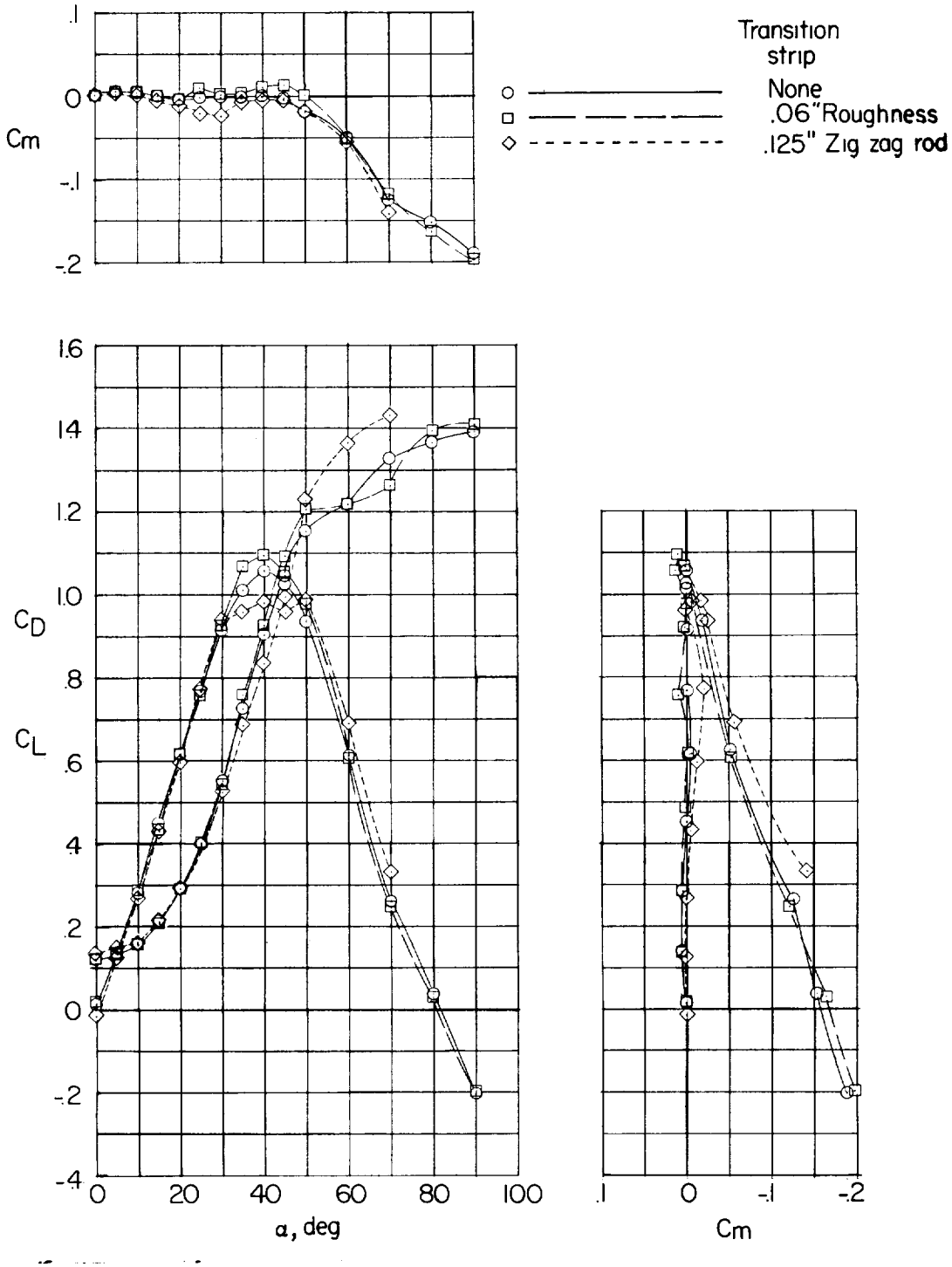

Figure 3.- Effect of transition strips on longitudinal characteristics of model 1.

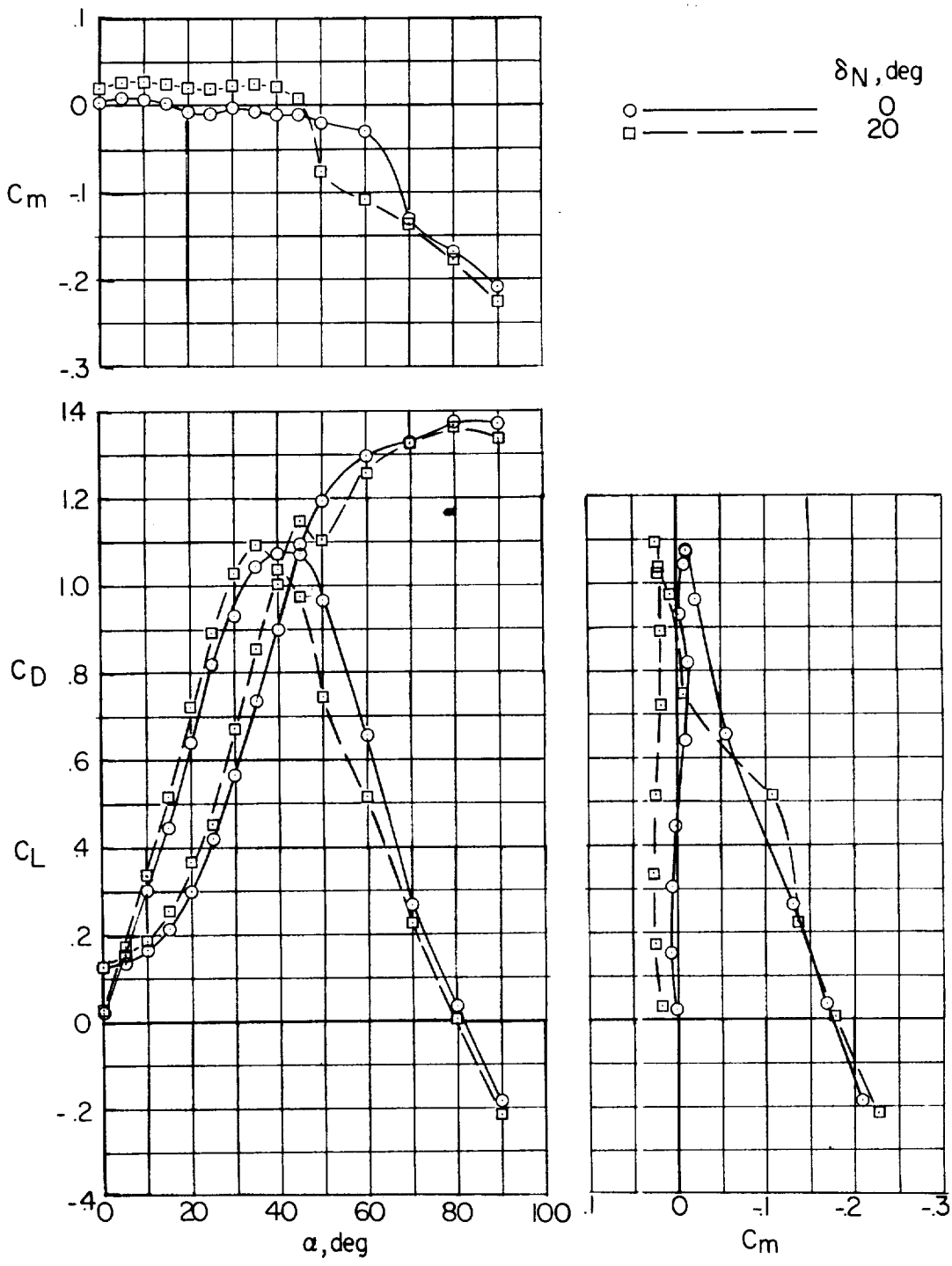

Figure 4.- Effect of nose deflection on longitudinal characteristics of model 1.

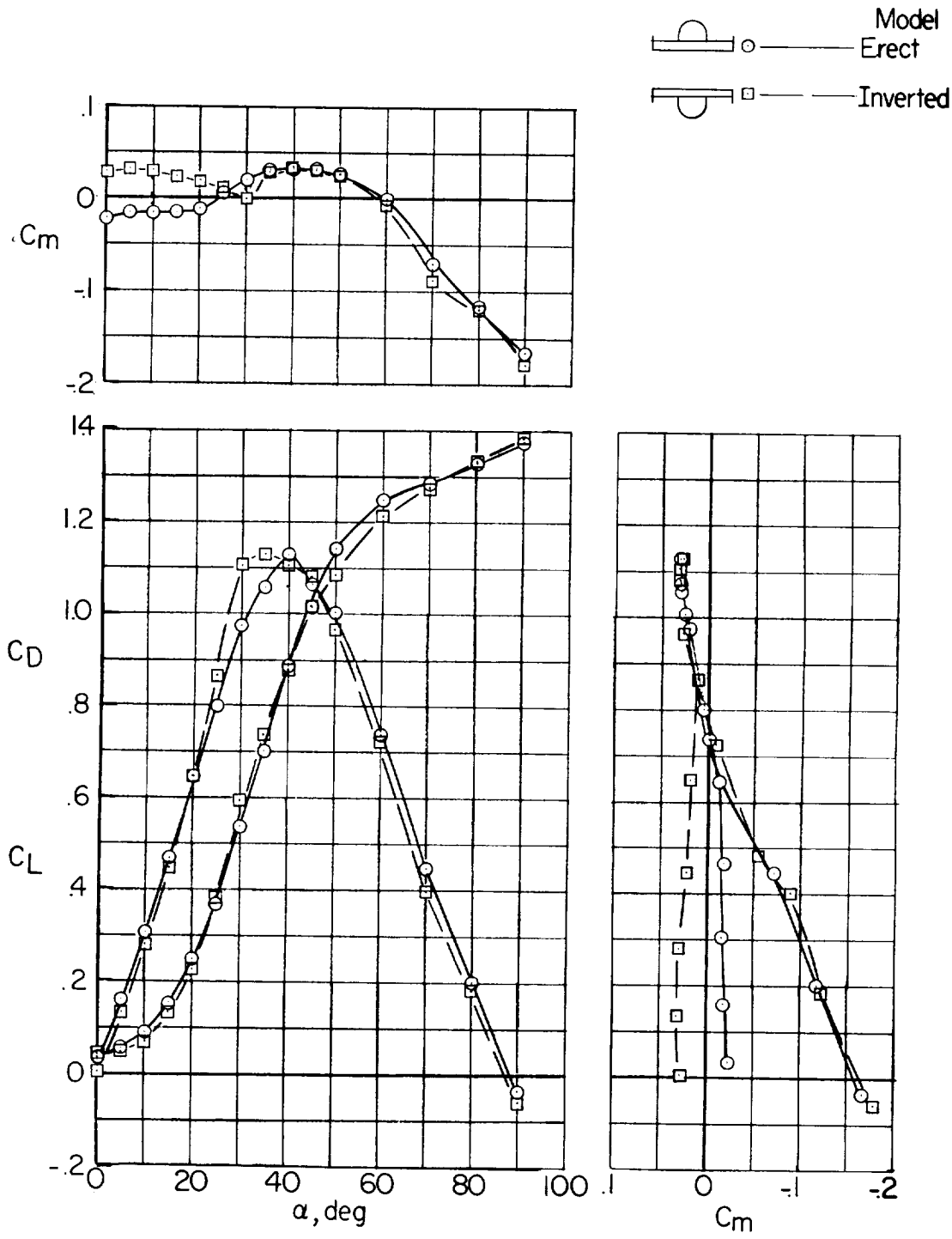

Figure 5.- Longitudinal characteristics of model 2.

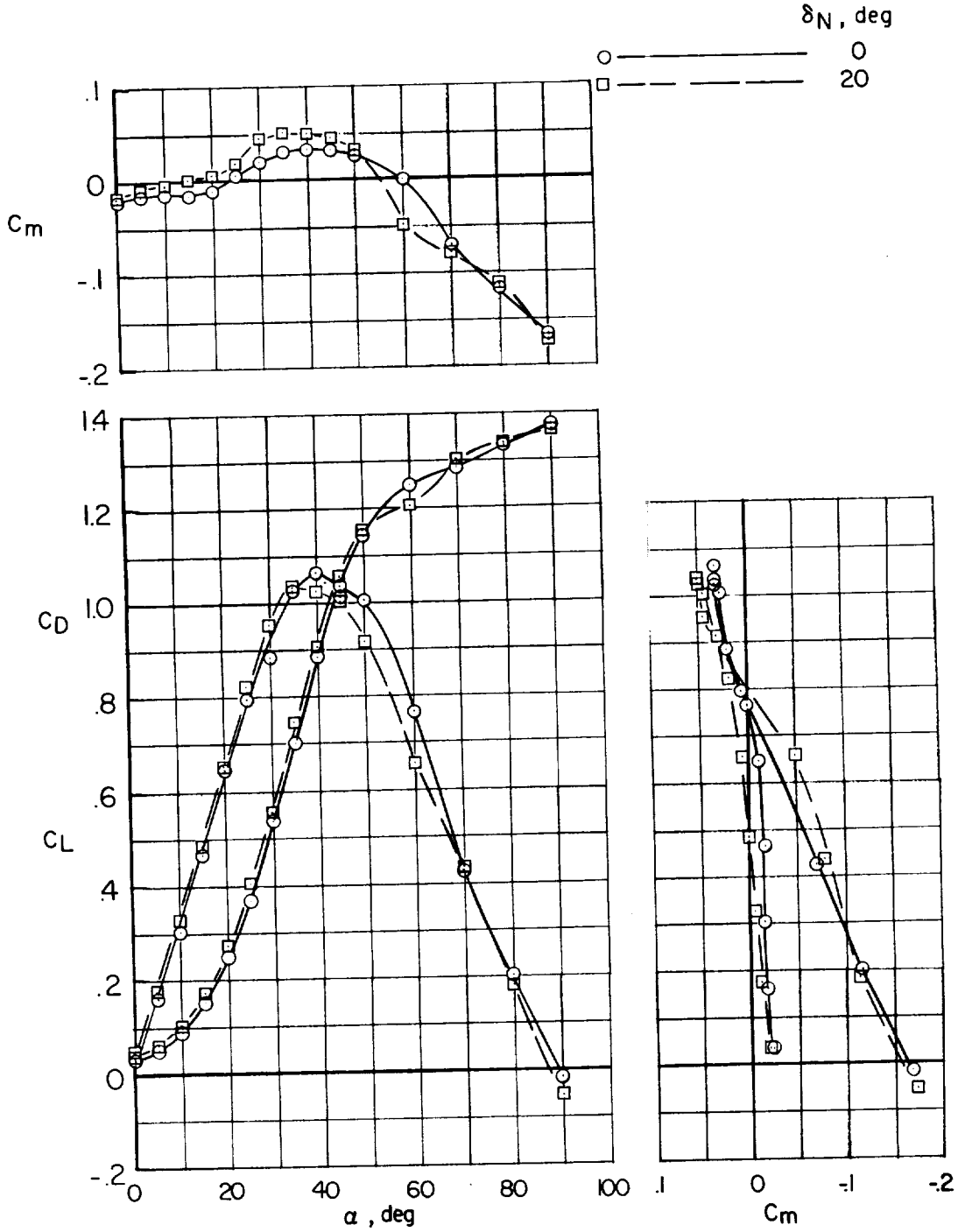

Figure 6.- Effect of nose deflection on longitudinal characteristics of model 2.

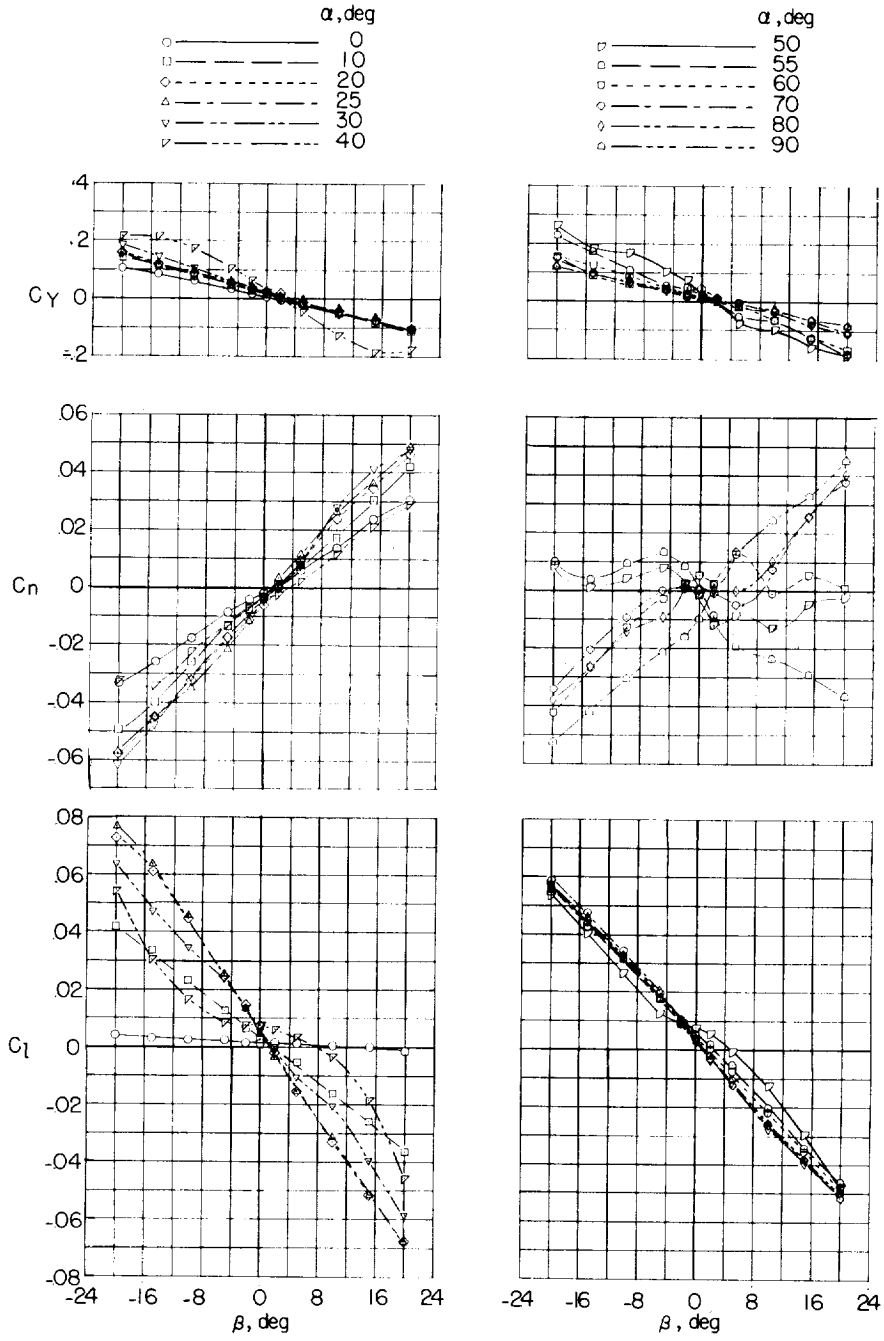

Figure 7.- Variation of static lateral stability characteristics with angle of sideslip for model 1.

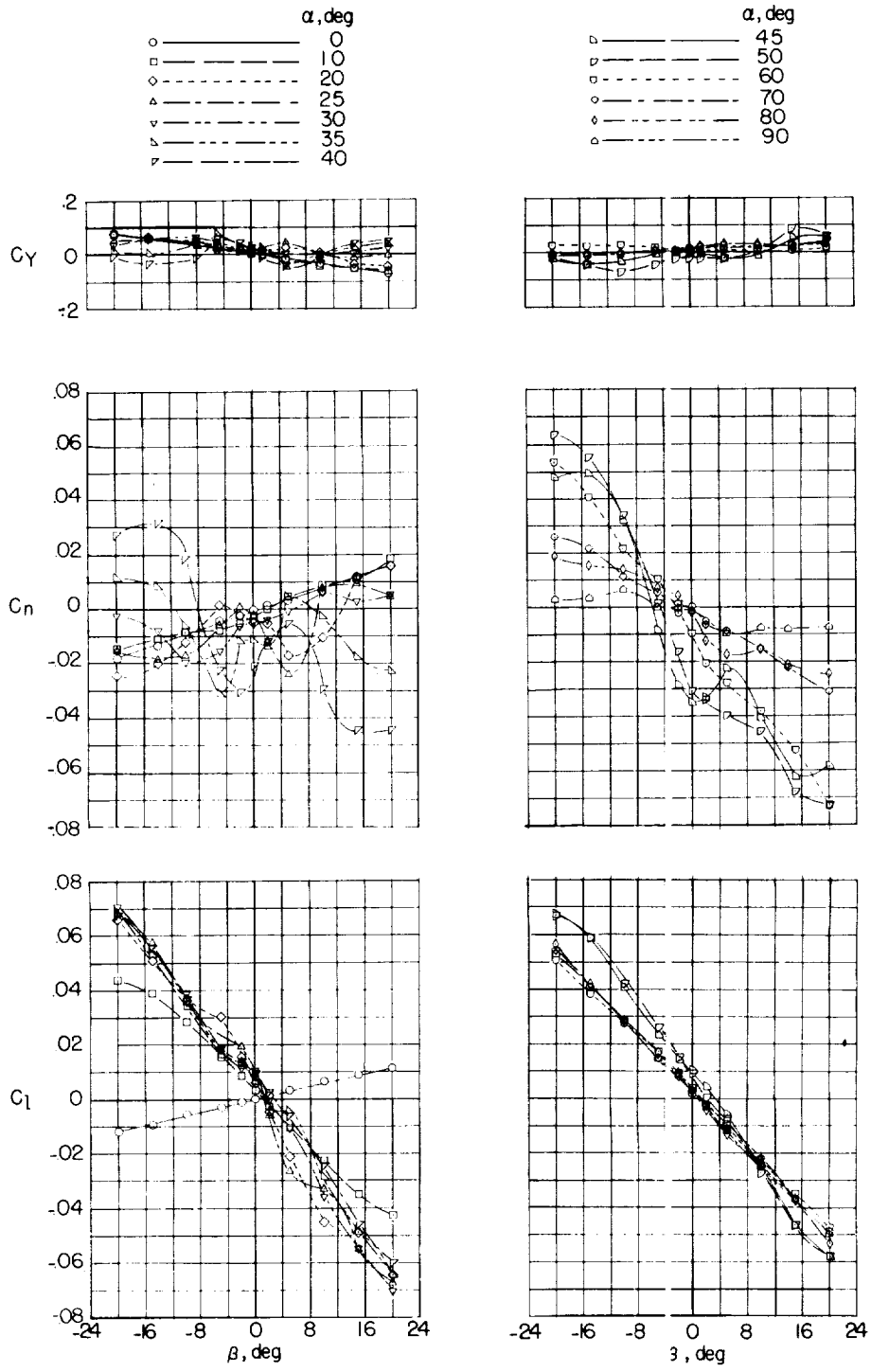

Figure 8.- Variation of static lateral stability characteristics with angle of sideslip for model 2. Model erect.

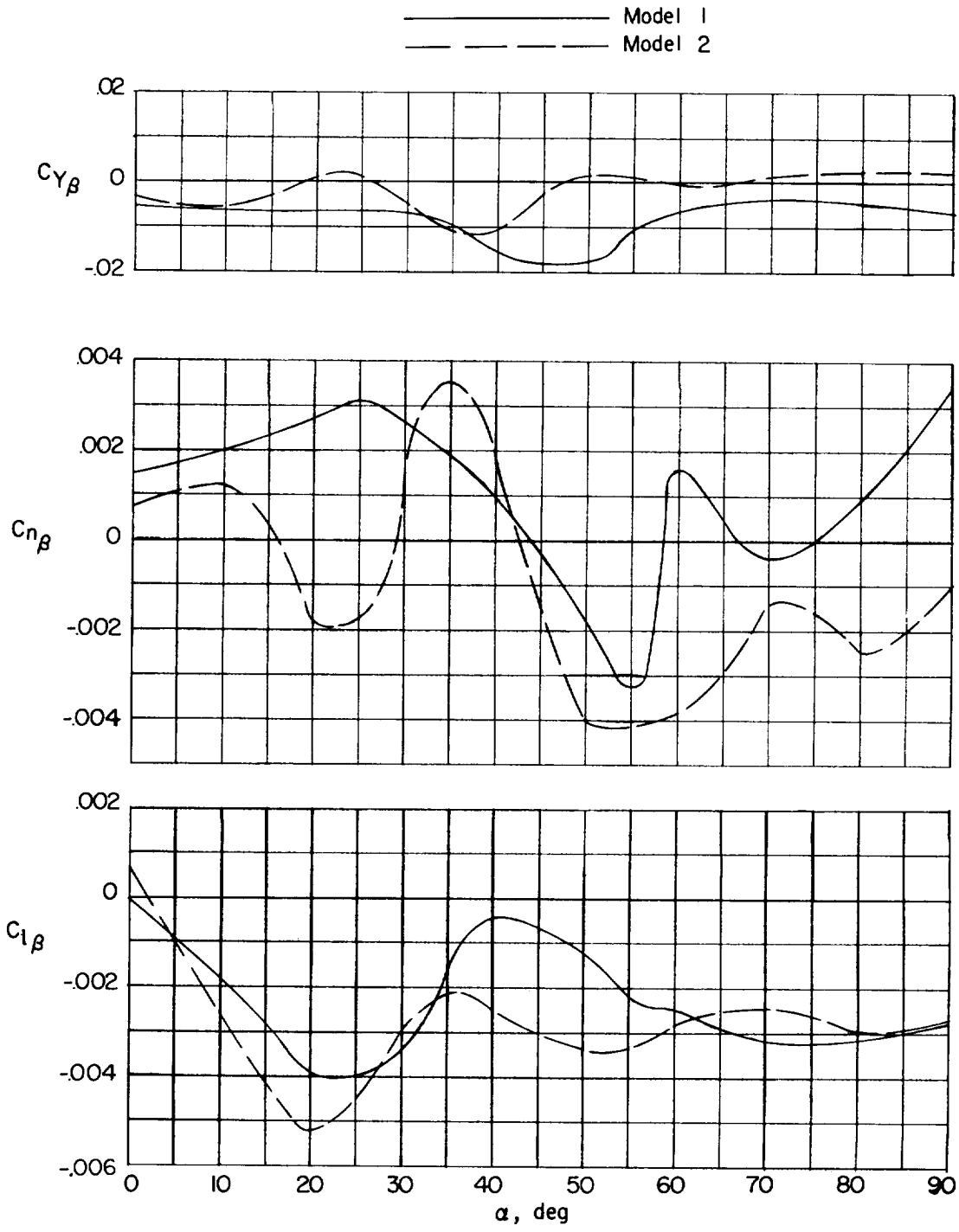

Figure 9.- Comparison of static sideslip characteristics of the basic models. $\beta = \pm 5^{\circ}$.

NASA - Langley Field, Va.